Molecular dynamics simulations of strongly coupled plasmas: Localization and microscopic dynamics[a)]

Z. Donkó[b)] and P. Hartmann
Research Institute for Solid State Physics and Optics of the Hungarian Academy of Sciences, P.O. Box 49, H-1525 Budapest, Hungary

G. J. Kalman
Department of Physics, Boston College, Chestnut Hill, Massachusetts 02467

(Received 7 November 2002; accepted 20 January 2003)

The spatial–temporal localization of particles in the local minima of the potential surface is a prominent feature of strongly coupled plasmas. The duration of localization is investigated by molecular dynamics simulation, through monitoring of the decorrelation of the surroundings of individual particles. Three- and two-dimensional systems of particles interacting through Coulomb and Yukawa potentials are studied over a wide range of the plasma coupling (Γ) and screening (κ) parameters in the liquid phase. The oscillation spectrum of the caged particles in the equilibrium system as well as in the frozen environment of other particles (Einstein frequency spectrum) is determined. © *2003 American Institute of Physics.* [DOI: 10.1063/1.1560612]

I. INTRODUCTION

The physics of strongly coupled plasmas has become a rapidly emerging field in the last few decades,[1] mostly due to its relevance to astrophysical plasmas, to rapidly progressing laboratory experiments on dusty plasmas,[2] and on cryogenically trapped cold plasmas.[3] Strongly coupled quasi-classical plasmas also occur in semiconductors.[4] In dusty plasmas the Coulomb interaction is screened by the oppositely charged particles (polarizable background), and the form of interaction follows the Yukawa potential:

$$\phi(r)=\frac{q^2\exp(-r/\lambda_D)}{r}, \tag{1}$$

where q is the charge of the particles and λ_D is the Debye (screening) length.

Depending on the configuration of the system, the particles may be located in three-dimensional (3-D) space or they can be confined to one or more two-dimensional (2-D) layer(s). Infinite model systems in their equilibrium state can be fully characterized by two dimensionless parameters: (i) the plasma coupling parameter

$$\Gamma=\frac{q^2}{ak_BT}, \tag{2}$$

and (ii) the screening parameter $\kappa=a/\lambda_D$, where T is the temperature and a is the Wigner–Seitz (WS) radius.[5,6] In 3-D and 2-D systems the WS radius is given by $a_{3\text{-}D}=(4n_{3\text{-}D}\pi/3)^{-1/3}$ and $a_{2\text{-}D}=(n_{2\text{-}D}\pi)^{-1/2}$, respectively, where $n_{3\text{-}D}$ and $n_{2\text{-}D}$ are the 3-D density and the 2-D surface density of particles. 3-D and 2-D one-component plasmas (OCPs) with $1/r$ Coulomb interaction potential represent the $\kappa=0$ case when the particles are immersed in a nonpolarizable (rigid) background of oppositely charged particles.

In dusty plasmas it is easy to achieve crystallization[7,8] due to the high charge of the dust particles (typically of the order of 10^3-10^4 electron charges). The crystalline state is evidently characterized by complete localization of particles. However, the localization of charged particles already shows up in the strongly coupled liquid phase.[9–12] Particles spend substantial periods of time in local minima of the rough potential surface that develops in such systems. At the same time, the time of localization is limited by the reformation of the potential surface due to the diffusion of the particles.

A theoretical approximation scheme based on the observation of localization is the quasi-localized charge approximation (QLCA) that has proven to be a very useful tool in theoretical studies of the properties of strongly coupled Coulomb and Yukawa systems.[13–15] In order for the QLCA to be valid one needs to assume that the period of time spent by the charges in the local potential minima extends over several oscillation cycles.

There are two major objectives addressed by the simulation work presented in this paper. The first relates to the quantitative formulation of the theoretically introduced notion of localization of particles. The principal issues here are the operationally meaningful definition of localization and the measurement of the localization time as a function of the plasma parameters in the strong coupling domain. The second objective is the exploration of the oscillation spectra of individual particles in different situations: in particular, we are interested both in the dynamical spectra and in the spectra generated by a single particle in the frozen environment of the other particles. While these questions in the ordered crystalline phase are fairly well understood, this is not the case in the disordered solid and even less in the strongly coupled liquid phase. Thus the data derived from the simu-

[a)]Paper QI2 6, Bull. Am. Phys. Soc. **47**, 251 (2002).
[b)]Invited speaker. Electronic mail: donko@sunserv.kfki.hu

lations should provide the foundation for the theoretical analysis of this problem. Studies along these lines have already been undertaken for the case of the 3-D OCP;[16] in this paper we extend our analysis to the 2-D OCP, as well as to systems with screened-Coulomb (Yukawa) interaction. In Sec. II of the paper we describe the simulation techniques. Section III presents the results derived from the simulations, while Sec. IV summarizes the work.

II. SIMULATION TECHNIQUE

The trajectories of particles are followed by molecular dynamics simulation, based on the particle–particle particle–mesh (PPPM) method,[17,18] using periodic boundary conditions. Both the 3-D and 2-D systems are simulated with a 3-D PPPM code, in the simulation of the 2-D system the particles are confined into a single plane (but their interaction remains three-dimensional). The number of particles is $N=1600$, at the start of the simulations random initial particle configurations are set, the initial velocities of the particles are sampled from a Maxwellian distribution with a temperature corresponding to the prescribed value of Γ. The system is thermostated for several thousand time steps, and the particle trajectories are traced typically for an additional several thousand time steps following the thermalization period.

In order to study the localization of particles we focus on the changes of the surroundings of individual particles, which is analyzed through the correlation techniques developed by Rabani *et al.*[19,20] The neighbors of a selected particle are defined as those situated within its first coordination shell [identified by the first minimum of the pair correlation function $g(r)$]. Following the formalism of Rabani *et al.*[19,20] a generalized neighbor list ℓ_i is defined for particle i as $\ell_i=\{f(r_{i,1}),f(r_{i,2}),\ldots,f(r_{i,N})\}$, where $f(r_{i,j})=\Theta(r_c-r_{i,j})$, Θ is the Heaviside function, i.e., $f=1$ if $r_{i,j}\leqslant r_c$, and $f=0$ otherwise. Here r_c is the cutoff radius, and the neighbors are said to be closely separated (and particle j is said to belong to the surrounding, or "cage" of particle i) if $r_{i,j}\leqslant r_c$.

The correlation between the surroundings of the particles at $t=0$ and t is measured by the "list correlation" function, derived from the scalar product of the neighbor list vectors:

$$C_\ell(t)=\frac{\langle \ell_i(t)\ell_i(0)\rangle}{\langle \ell_i(0)^2\rangle}, \tag{3}$$

where $\langle . \rangle$ denotes averaging over particles and initial times. The number of particles that have left the original cage of particle i at time t can be determined as

$$n_i^{\mathrm{out}}(0,t)=|\ell_i(0)^2|-\ell_i(0)\ell_i(t), \tag{4}$$

where the first term gives the number of particles around particle i at $t=0$, while the second term gives the number of "original" particles that remained in the surrounding after time t elapsed. The cage correlation function C_{cage} that characterizes the decay of the cages can be calculated for different number of particles, c, leaving the cage, as an ensemble and time average of the function $\Theta(c-n_i^{\mathrm{out}})$:

$$C_{\mathrm{cage}}^{(c)}(t)=\langle \Theta(c-n_i^{\mathrm{out}}(0,t))\rangle. \tag{5}$$

We call the cages decorrelated when the $C_{\mathrm{cage}}^{(c)}(t)$ function (with c being set to the half of the average number of neighbors, i.e., $c=7$ in 3-D and $c=3$ in 2-D) decays to 0.1. In other words, the decorrelation time t_{decorr} is defined as $C_{\mathrm{cage}}^{(7)}(t_{\mathrm{decorr}})=0.1$ in 3-D and $C_{\mathrm{cage}}^{(3)}(t_{\mathrm{decorr}})=0.1$ in 2-D.

The oscillation frequencies of selected particles are analyzed both in the system in dynamical equilibrium, as well as in the frozen environment of other particles (yielding the Einstein frequency).

In the equilibrium system in the high-coupling domain the p_x-x phase space trajectories of individual particles have been found to include characteristic loops, representing caged particles.[16] Such loops are searched for in the collection of the phase space trajectories recorded during the simulation of the equilibrium ensemble, and then the frequencies associated with their characteristic times are calculated. Finally a histogram of these frequencies is obtained for each Γ and κ.

The Einstein frequencies of a system are defined[21] as the 3 (in 3-D) or 2 (in 2-D) eigenfrequencies ($\omega_{\mathrm{E}i}$, $i=1, 2, 3$ in 3-D and $i=1, 2$ in 2-D) of an oscillating particle around its quasi-equilibrium position in the potential generated by the frozen environment of the other particles. Thus, in the simulations aimed at the determination of the Einstein frequency, all but the selected particle are immobilized at a certain instant. Then the simulation proceeds for a given number of additional time steps and the trajectory of the freely moving particle is recorded. The system is subsequently thermalized for 1000 time steps and the experiment is repeated several times. The $x(t)$, $y(t)$, and $z(t)$ trajectories, recorded during the experiments, are frequency analyzed and a histogram is constructed from the 3 (2) peaks of the spectra. In each run, the characteristic frequency $\Omega_{\mathrm{E}}=(\Sigma_i\omega_{\mathrm{E}i}^2)^{1/2}$ is also recorded and a histogram for Ω_{E} is constructed, as well. The $\omega_{\mathrm{E}i}$ data obtained from individual runs also make it possible to calculate the average Einstein frequency $\overline{\omega}_{\mathrm{E}}=(\langle\omega_{\mathrm{E}i}^2\rangle)^{1/2}$.

III. RESULTS

A. Localization (caging)

To illustrate the appearance of the potential surface, Fig. 1 shows a snapshot of the potential distribution in a plane of a 3-D OCP at $\Gamma=160$. If a test particle is located in any of the potential minima (shown by dark color), it is evidently momentarily trapped. To quantify the duration of trapping (localization) we make use of the correlation techniques presented in Sec. II, by calculating the cage correlation functions.

The behavior of the cage correlation functions is illustrated for the 2-D system. Figure 2(a) shows the $C_{\mathrm{cage}}^{(3)}$ functions for a series of Γ values, for the Coulomb case ($\kappa=0$) while Fig. 2(b) displays the dependence of the cage correlation function of κ for constant Γ. The cage correlation functions are plotted against the dimensionless time, $T=\omega_p t/2\pi$ (equal to the number of plasma oscillation cycles). For the 3-D system the plasma frequency is given by $\omega_p=(4\pi n_{3\text{-D}}q^2/m)^{1/2}$, while in 2-D $\omega_p=(2\pi n_{2\text{-D}}q^2/ma_{2\text{-D}})^{1/2}$. As can be seen in Figs. 2(a) and 2(b), both the

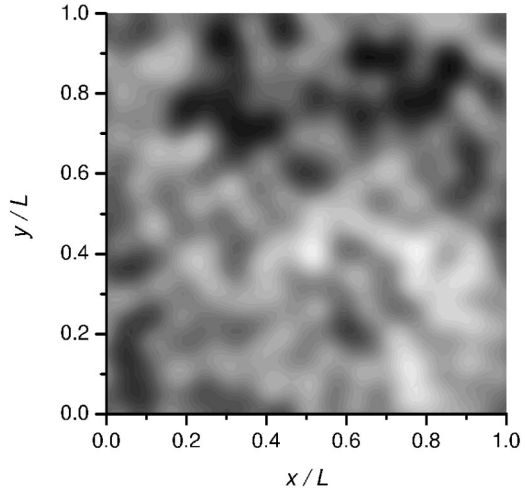

FIG. 1. Snapshot of a 2-D section of the potential surface in a 3-D OCP at $\Gamma = 160$. Light and dark shades indicate high and low values of the potential, respectively.

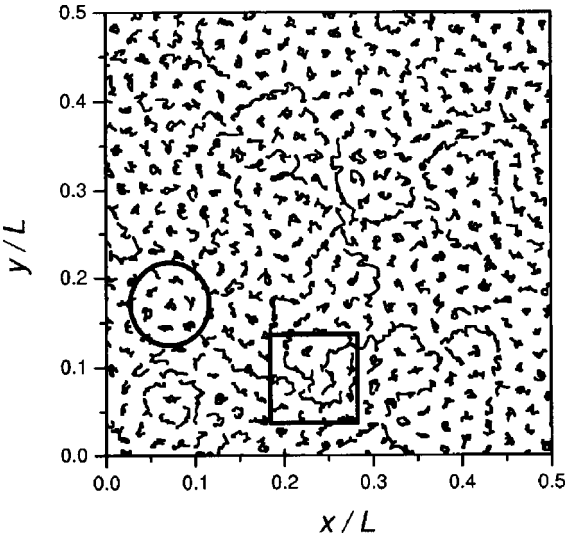

FIG. 3. Trajectory segments in a 2-D Yukawa system at $\Gamma = 120$ and $\kappa = 1$ recorded for $\Delta T = \omega_p \Delta t / 2\pi \approx 6.5$. The circle shows a region with strong caging, while the square shows a region characterized by significant migration of the particles. (Only one quarter of the simulation box is shown.)

decreasing Γ and the increasing screening (κ) result in a shorter-time decay of the cage correlation function.

It is noted that the cage correlation functions represent the average behavior of the cages as prescribed by the definition (5). On the other hand, one can also monitor the decorrelation of individual cages. Such a study, as done for the 3-D OCP[16] indicated that the decorrelation time has a broad distribution for any given set of system parameters. This behavior can also be identified from the plot of trajectory segments plotted in Fig. 3 obtained in a 2-D Yukawa system (at $\Gamma = 120$ and $\kappa = 1$). The plot clearly shows some regions where the localization is almost complete during the time of the recording ($\omega_p \Delta t / 2\pi \approx 6.5$), while in other regions a significant migration of the particles is observed. This behavior may also be related to the recent experimental observations[22] (in a 2-D Yukawa plasma) where some of the particles were found to be caged for a long time, while others moved relatively freely in the system.

The dimensionless decorrelation time $T_{\mathrm{decorr}} = \omega_p t_{\mathrm{decorr}} / 2\pi$ (with t_{decorr} defined in Sec. II) is shown as a function of

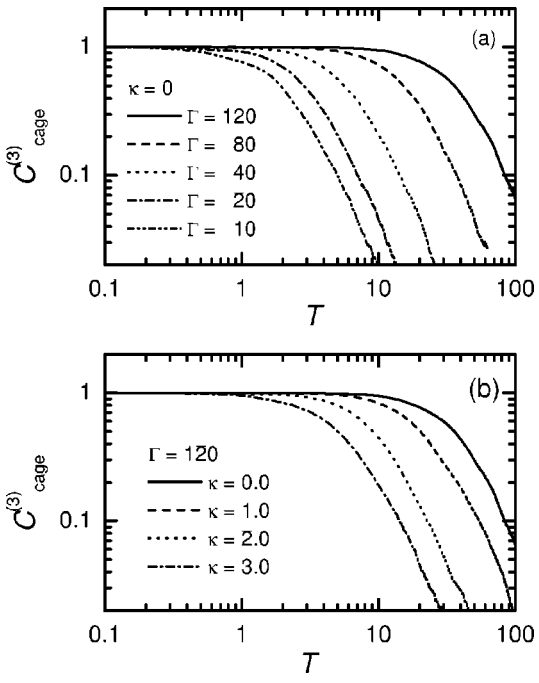

FIG. 2. Cage correlation functions $C^{(3)}_{\mathrm{cage}}$ for the 2-D system. (a) Dependence on Γ at $\kappa = 0$, (b) dependence on κ at $\Gamma = 120$.

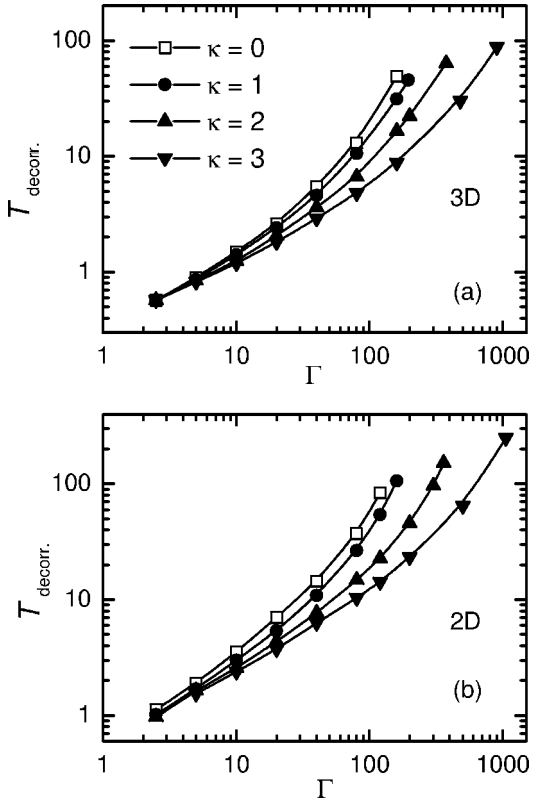

FIG. 4. Decorrelation time of the cages as a function of Γ for the (a) 3-D and (b) 2-D systems, for a series of κ values.

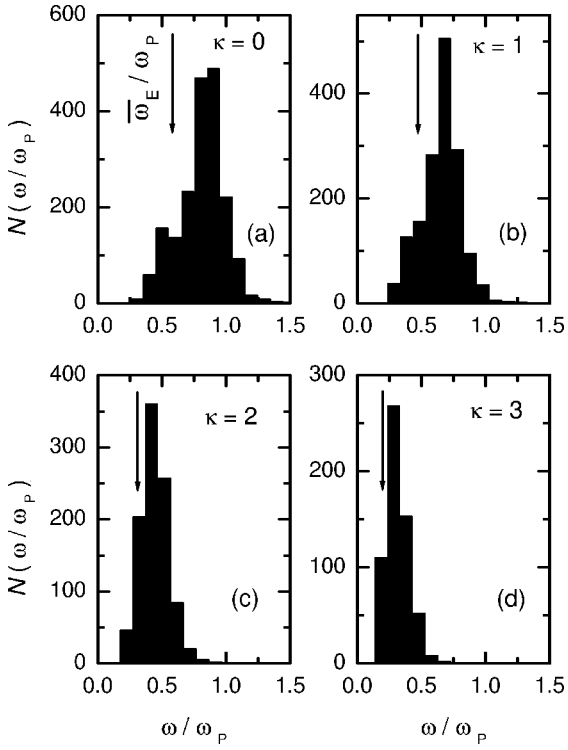

FIG. 5. Histogram of frequencies obtained from nearly closed trajectory segments of caged particles in the 3-D equilibrium system at $\Gamma=160$ and a series of κ values. N is the number of events a particular oscillation frequency has been observed. The arrows mark the position of the average Einstein frequency $\bar{\omega}_E$.

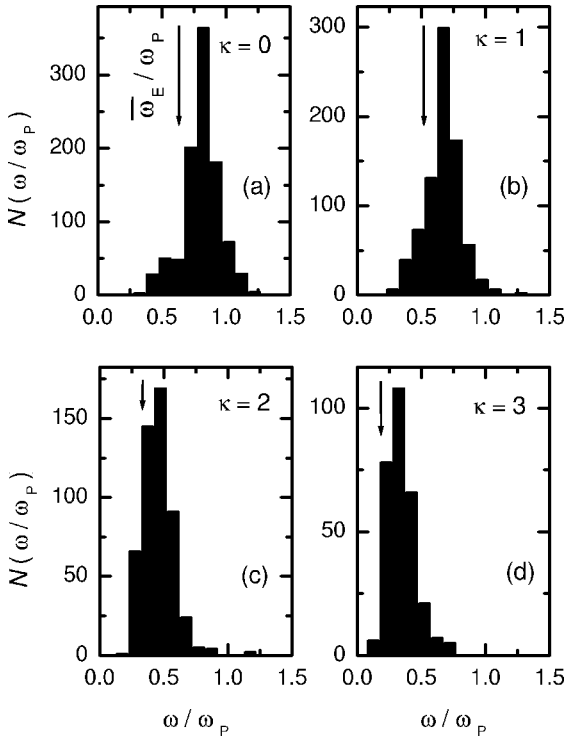

FIG. 6. Histogram of frequencies obtained from nearly closed trajectory segments of caged particles in the 2-D equilibrium system at $\Gamma=120$ and a series of κ values. N is the number of events a particular oscillation frequency has been observed. The arrows mark the position of the average Einstein frequency $\bar{\omega}_E$.

Γ for a series of κ values in Figs. 4(a) and 4(b), for 3-D and 2-D systems, respectively.

In the case of the 3-D system, at $\kappa=0$ and $\Gamma=160$ the cages decorrelate during ≈ 50 plasma cycles. The decorrelation time is shortened to a single cycle at $\Gamma\approx 7$. In the case of the 2-D system it takes about 100 cycles for the cages to decorrelate at $\kappa=0$ and $\Gamma=120$, and we reach $T_{\mathrm{decorr}}=1$ at $\Gamma\approx 2.5$. In the high-Γ domain we observe a strong dependence of the decorrelation time on κ for $\kappa\geqslant 0.4$, both in 3-D and 2-D systems. At low values of Γ, however, T_{decorr} depends only slightly on κ. (For $\kappa<0.4$ there is a very weak dependence of the results on the value of κ for the whole range of Γ.) The decrease of the decorrelation time for increasing κ can be compensated by increasing Γ, as can be seen in Fig. 4.

The results presented in Fig. 4 indeed confirm the basic assumption of the QLCA method that in the strong coupling domain the localization time of the particles largely exceeds the period of plasma oscillations.

B. Frequency spectra (Ref. 23)

The frequency spectra of the oscillation of caged particles is analyzed by identifying loops in the p_x-x (and p_y-y, p_z-z) phase planes. These loops represent quasilocalized (bounded) motion of particles; once these segments have been identified and segregated, a frequency histogram of the oscillation frequencies associated with their characteristic times is readily obtained. The frequency histograms are displayed in Fig. 5 for the 3-D system at $\Gamma=160$. At $\kappa=0$ [Fig. 5(a)] the oscillation frequency scatters roughly between the plasma frequency ω_p and the average Einstein frequency $\bar{\omega}_E=(\langle\omega_{Ei}^2\rangle)^{1/2}$ which also marks the $k\to\infty$ limit of the collective mode frequency in the QLCA.[15] For $\kappa>0$, the entire spectrum gradually shifts toward lower frequencies as κ increases; this is shown in Figs. 5(b), 5(c), and 5(d) for $\kappa=1$, 2, and 3, respectively. The frequency spectra of the 2-D system, as shown in Figs. 6(a)–6(d) (plotted for $\Gamma=120$), have a similar appearance.

In order to highlight the effect of the dynamical interaction between the particles on the frequency spectrum we have also analyzed the distribution of the Einstein frequencies by immobilizing all the particles except the one whose spectrum is observed. A series of frequency histograms obtained at $\Gamma=160$ and different values of the screening parameter κ is shown in Fig. 7 for the 3-D system. The frequency spectra are relatively sharp, compared to the dynamical spectrum. The peak of the histograms shifts to lower frequency as κ increases. It is noted that at lower values of Γ the frequency distributions become wider. This may be due to the fact that at lower coupling there is increasing randomness of particle positions and, consequently, increasing deviation from spherical symmetry in the environment sampled by the oscillating charge. Similar Einstein frequency histograms for 2-D systems at $\Gamma=120$ are shown in Fig. 8.

Further understanding of the physical origin of the Einstein spectra can be derived from the observation of the relationships between the oscillation frequencies of a particle

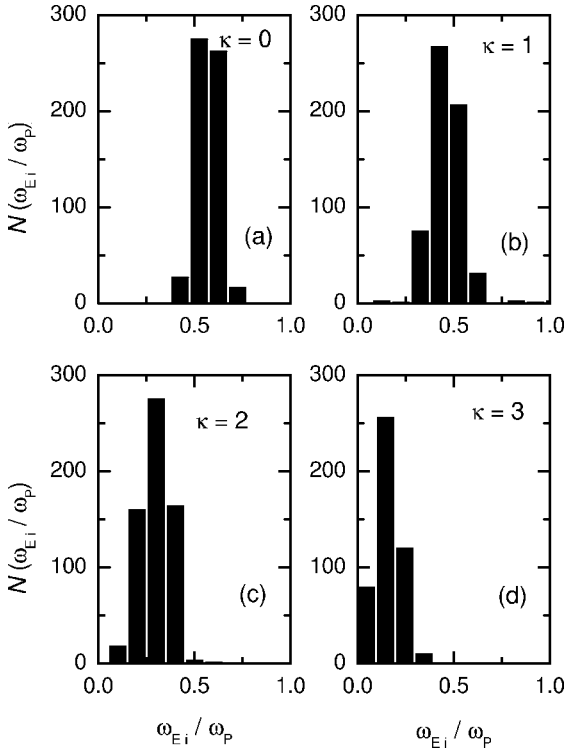

FIG. 7. Histogram of Einstein frequencies obtained from the oscillation of single caged particles in the frozen environment of the other particles in the 3-D system at $\Gamma=160$ and a series of κ values. N is the number of events where Einstein frequencies ω_{Ei} have been observed.

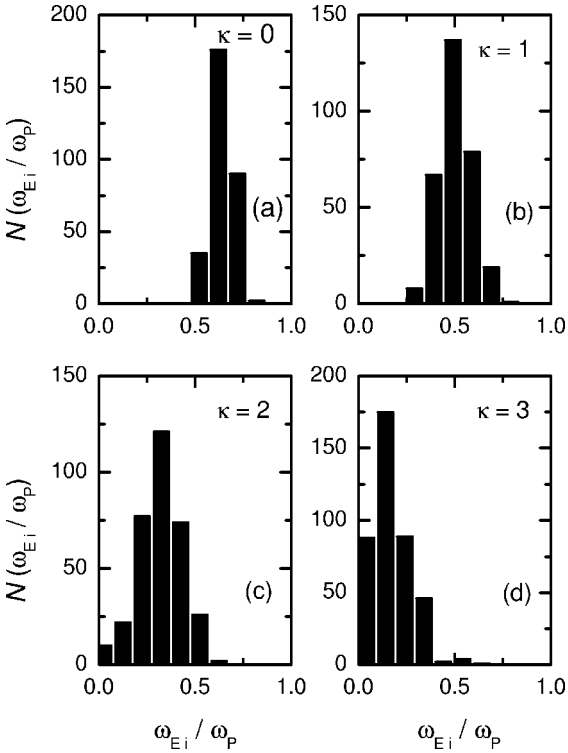

FIG. 8. Histogram of Einstein frequencies obtained from the oscillation of single caged particles in the frozen environment of the other particles in the 2-D system at $\Gamma=120$ and a series of κ values. N is the number of events where Einstein frequencies ω_{Ei} have been observed.

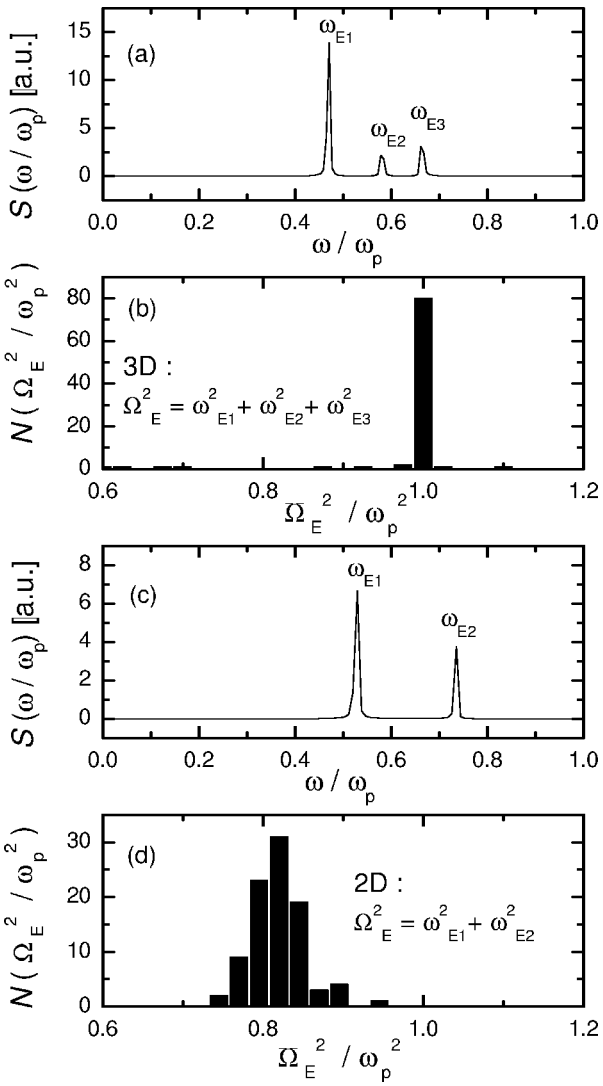

FIG. 9. Sample of frequency spectra $S(\omega/\omega_p)$ for individual runs and histograms of Ω_E^2/ω_p^2 in 3-D (a),(b) and in 2-D (c),(d) at $\kappa=0$. ω_{Ei} are the Einstein (eigen)frequencies observed in a single simulation run. (a),(b): $\Gamma=160$; (c),(d) $\Gamma=20$.

in an individual run.[24] In 3-D there are three such frequencies (ω_{Ei}), as illustrated in Fig. 9(a). These frequencies appear in the vicinity of $\overline{\omega}_E$. The scattering of the frequencies around $\overline{\omega}_E$ is governed by the prevailing disorder. The value of $\overline{\omega}_E$ in a 3-D Coulomb system ($\kappa=0$) is dictated by the Kohn sum rule (KSR)[25,13] that requires that in each run $\Omega_E^2=\omega_p^2$: consequently in 3-D $\overline{\omega}_E=\omega_p/\sqrt{3}$ [see Fig. 9(b)]. In 2-D there are two frequencies [see Fig. 9(c)] and since the KSR does not apply, Ω_E^2 follows a distribution: the ensuing qualitative difference is well illustrated in Fig. 9(d).

The average Einstein frequency $\overline{\omega}_E$ as a function of κ is shown in Fig. 10 for 3-D and 2-D systems. At $\kappa=0$ we have a very good agreement with the theoretical values for the 3-D system: $\overline{\omega}_E/\omega_p=1/\sqrt{3}\cong 0.577$, and for the 2-D system: $\overline{\omega}_E/\omega_p=0.642$.[13–15] Both the 3-D and 2-D systems exhibit a distinct drop of $\overline{\omega}_E$ as κ increases. The data obtained for the 3-D system are in good agreement (except at $\kappa=3$) with the results of the QLCA theory, which is also shown in Fig. 10. The reason for the disagreement at high κ values is not well understood, but it may be due to the inadequacy of the hy-

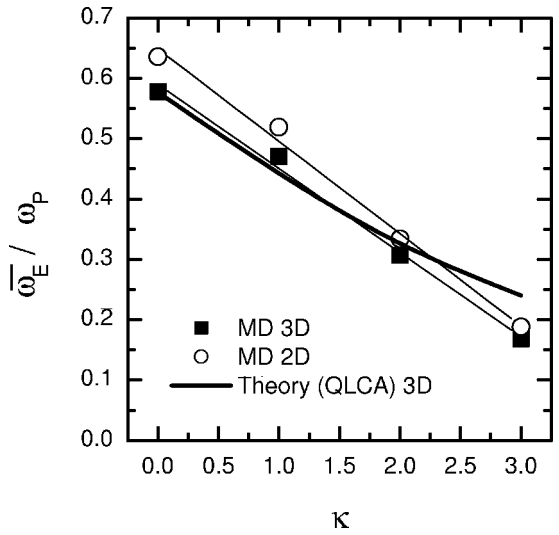

FIG. 10. Mean Einstein frequency as obtained from the MD simulations for the 3-D and 2-D systems (symbols), and the prediction of the QLCA theory for the 3-D system (heavy line). $\Gamma = 160$ for 3-D and $\Gamma = 120$ for 2-D.

pernetted chain generated pair correlation functions used as an input in the QLCA calculations.

IV. SUMMARY

In this paper we have obtained quantitative information about the localization of particles in strongly coupled Coulomb and Yukawa plasmas by analyzing through molecular dynamics simulation the dependence of the particle dynamics on the coupling Γ and screening κ parameters. The simulation results support the physical basis of the QLCA; at high values of Γ the particles are caged by their nearest neighbors and spend several oscillation cycles in local minima of the rough potential surface without experiencing substantial changes in their surroundings. The caging time is a fast growing function of Γ; it decreases, however, with increasing κ. The caged particles exhibit a characteristic oscillation spectrum. The mean oscillation frequency of the caged particles has been found to decrease with increasing κ both in the equilibrium system and in the frozen environment of the other particles.

Our ability to theoretically describe the results obtained is rather limited. While the localization of particles in the strong coupling domain was predicted on theoretical grounds,[13] the understanding of the crucial Γ dependence of the caging time and of the difference between 3-D and 2-D scenarios is lacking. The problem of the distribution of the Einstein frequencies (Figs. 7 and 8) in topologically disordered systems has been a long-standing problem of condensed matter physics:[21] in the present context it is further compounded by difficulties associated with the long-range character of the Coulomb interaction and the issue of dimensionality in this connection. As to the dynamical spectra (Figs. 5 and 6), their connection with the frequency spectrum generated by the dynamical structure function $S(k,\omega)$ should be further explored: a better understanding of this relationship may lead to an improved description of the collective mode structure in disorder dominated strongly coupled plasmas.

ACKNOWLEDGMENTS

Useful discussions with Kenneth Golden and Pradip Bakshi are gratefully acknowledged.

Financial support through Grant Nos. OTKA-T-34156 and MTA-NSF-OTKA-028 is gratefully acknowledged; the work has also been partially supported by NSF Grant No. INT-0002200 and DOE Grant No. DE-FG02-98ER54501.

[1] For most recent general references see *Proceedings of the International Conference on Strongly Coupled Coulomb Systems, Santa Fe, NM, September 2002*, edited by J. Dufty, J. F. Benage, and M. S. Murillo (IOP, Bristol, 2003), in press.
[2] M. Zuzic, A. V. Ivlev, J. Goree *et al.*, Phys. Rev. Lett. **85**, 4064 (2000); S. Nunomura, D. Samsonov, and J. Goree, *ibid.* **84**, 5141 (2000).
[3] J. J. Bollinger, D. J. Wineland, and D. H. E. Dubin, Phys. Plasmas **1**, 1403 (1994); T. B. Mitchell, J. J. Bollinger, D. H. E. Dubin, X.-P. Huang, W. M. Itano, and R. H. Bundham, Science **282**, 1290 (1998).
[4] See, e.g., S. Shapira, U. Sivan, P. M. Solomon, E. Buchstab, M. Tischlerand, and G. Ben Yosef, Phys. Rev. Lett. **77**, 3181 (1996).
[5] M. Baus and J.-P. Hansen, Phys. Rep. **59**, 1 (1980).
[6] S. Ichimaru, Rev. Mod. Phys. **54**, 1017 (1982).
[7] R. T. Farouki and S. Hamaguchi, J. Chem. Phys. **101**, 9885 (1994).
[8] S. Hamaguchi, R. T. Farouki, and D. H. E. Dubin, J. Chem. Phys. **105**, 7641 (1996).
[9] J.-P. Hansen, Phys. Rev. A **8**, 3096 (1973); E. Pollock and J.-P. Hansen, *ibid.* **8**, 3110 (1973).
[10] W. L. Slattery, G. D. Doolen, and H. E. DeWitt, Phys. Rev. A **21**, 2087 (1980); **26**, 2255 (1982).
[11] S. Ogata and S. Ichimaru, Phys. Rev. A **36**, 5451 (1987); **39**, 1333 (1989); J. Phys. Soc. Jpn. **58**, 356 (1989).
[12] G. S. Stringfellow, H. E. DeWitt, and W. L. Slattery, Phys. Rev. A **41**, 1105 (1990).
[13] G. J. Kalman and K. I. Golden, Phys. Rev. A **41**, 5516 (1990).
[14] K. I. Golden, G. J. Kalman, and Ph. Wyns, Phys. Rev. A **46**, 3454 (1992).
[15] K. I. Golden and G. J. Kalman, Phys. Plasmas **7**, 14 (2000).
[16] Z. Donkó, G. J. Kalman, and K. I. Golden, Phys. Rev. Lett. **88**, 225001 (2002).
[17] R. W. Hockhey and J. W. Eastwood, Comput. Phys. Commun. **19**, 215 (1980).
[18] R. W. Hockhey and J. W. Eastwood, *Computer Simulation Using Particles* (McGraw–Hill, New York, 1981).
[19] E. Rabani, J. D. Gezelter, and B. J. Berne, J. Chem. Phys. **107**, 6867 (1997).
[20] E. Rabani, J. D. Gezelter, and B. J. Berne, Phys. Rev. Lett. **82**, 3649 (1999).
[21] A. Czahor, Acta Phys. Pol. A **69**, 281 (1986).
[22] Y.-J. Lai and L. I, Phys. Rev. Lett. **89**, 155002 (2002).
[23] This segment of the work has been carried out in collaboration with P. Bakshi.
[24] P. Bakshi, Z. Donkó, and G. J. Kalman, "Einstein frequency distributions for strongly coupled plasmas," Invited paper, to be presented at the 11th International Workshop on the Physics of Nonideal Plasmas (PNP 11), Valencia, Spain, 20–25 March 2003.
[25] R. A. Caldwell-Horsfall and A. A. Maradudin, J. Math. Phys. **1**, 395 (1960).